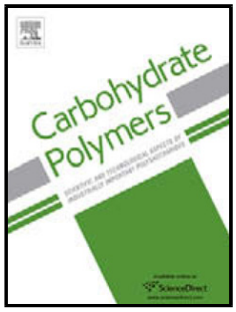

Title: An arabinogalactan from flowers of *Panax notoginseng* inhibits angiogenesis by BMP2/Smad/Id1 signaling

Author: Peipei Wang Lei Zhang Jian Yao Yikang Shi Ping Li Kan Ding

PII: S0144-8617(14)01216-8
DOI: http://dx.doi.org/doi:10.1016/j.carbpol.2014.11.073
Reference: CARP 9523

To appear in:

Received date: 30-9-2014
Revised date: 26-11-2014
Accepted date: 29-11-2014

Please cite this article as: Wang, P., Zhang, L., Yao, J., Shi, Y., Li, P., and Ding, K.,An arabinogalactan from flowers of *Panax notoginseng* inhibits angiogenesis by BMP2/Smad/Id1 signaling, *Carbohydrate Polymers* (2015), http://dx.doi.org/10.1016/j.carbpol.2014.11.073

An arabinogalactan from flowers of *Panax notoginseng* inhibits angiogenesis by BMP2/ Smad/Id1 signaling

Peipei Wang[#, 1, 2], Lei Zhang[#, 1, 2], Jian Yao[2], Yikang Shi[3], Ping Li*[, 1] and Kan Ding*[, 2]

[1] *State Key Laboratory of Natural Medicines and Department of Pharmacognosy, China Pharmaceutical University, Nanjing, 210009, China*

[2] *Glycochemistry & Glycobiology Lab, Shanghai Institute of Materia Medica, Chinese Academy of Sciences, Shanghai,201203,China*

[3]*National Glycoengineering Research Center，Shandong University*

[#]P. W. and L. Z. contributed equally to this work.

* Corresponding author

Glycochemistry & Glycobiology Lab, Shanghai Institute of Materia Medicca, Chinese Academy of Sciences, 555 Zu Chong Zhi Road, Pudong, Shanghai 201203, P.R. of China.

Tel./Fax: +86 21 50806928. dingkan@simm.ac.cn (Dr. Kan. Ding).

State Key Laboratory of Natural Medicines and Department of Pharmacognosy, China Pharmaceutical University, No. 24 Tongjia Lane, Nanjing 210009, China.

Tel./Fax: +86 25 83271379. liping2004@126.com (Dr. Ping Li)

Abstract: Angiogenesis plays an essential role in tumor development. Blocking angiogenesis in tumor has become a promising tactic in limiting cancer progression. Here, an arabinogalactan polysaccharide, RN1 was isolated from flowers of *Panax notoginseng*. Its structure was determined to possess a backbone of 1,6-linked Gal*p* branched at C3 by side 1,3-linked Gal*p*, with branches attached at position O-3 of it. The branches mainly contained 1,5-linked, 1,3,5 linked, terminal Arabinose and terminal Galactose. RN1 could inhibit microvessel formation in the BxPC-3 pancreatic cancer cell xenograft tumor in nude mice. The antiangiogenesis assay showed that RN1 could reduce the migratory activity of endothelial cells and their ability of tube formation on matrigel, but no effect on endothelial cells growth. Further studies revealed that RN1 could inhibit BMP2/ Smad1/5/8/Id1 signaling. All those data indicated the RN1 had an antiangiogenic effect via BMP2 signaling and could be a potential novel inhibitor of angiogenesis.

.

Key words：Arabinogalactan; *Panax notoginseng*; antiangiogenesis; BMP2

1. INTRODUCTION

Angiogenesis is a physiological process involving the growth of new blood vessels from existing vessels. It is now widely recognized as one of the hallmarks of cancer, a crucial step in the transition of tumors from a dormant state to a malignant state, and playing an essential role in tumor growth, invasion and metastasis (Folkman & Shing, 1992; Hanahan & Weinberg, 2011). Due to its essential roles in tumor, controlling tumor-associated angiogenesis has become a promising tactic in limiting cancer progression (Weis & Cheresh, 2011).

Our group has been actively involved in the search for new modulators of angiogenesis from natural products. We have reported that sulfate polysaccharide WSS25 (Qiu, Yang, Pei, Zhang & Ding, 2010) inhibited angiogenesis by binding to bone morphogenetic protein 2 (BMP2), a pro-angiogenesis protein. However, in the animal safety experiment, we found that WSS25 could increase the chances of internal bleeding at its high concentration. Thus development of safe and effective potential drug is essential.

The flowers of *Panax notoginsen* (FPN) has been wildly used as a traditional Chinese medicine and food additives. Recent study showed that the extract of flowers from *Panax notoginsen* had strong anti-proliferative effects on colorectal cancer cells (Ng, 2006). Here, in the course of a screening program, RN1, firstly isolated and purified from FPN, was selected for its ability to inhibit angiogenesis *in vitro* and *in vivo*. To our knowledge, the structure of arabinogalactan RN1 and its antiangiogenesis activity from FPN have not been reported previously.

2. MATERIAL AND METHODS

2.1. Materials

The dried flowers of *Panax notoginseng* were purchased from shanghaikangqiao Co., Ltd., Shanghai, China and were identified by Prof. Ping Li (Department of Pharmacognosy, China Pharmaceutical University, Nanjing, China). Monosaccharide standards (galactose, glucose, mannose, arabinose, xylose, rhamnose, galacturonic

acid) were all from Fluka, Switzerland. Trifluoroacetic acid (TFA), 1-phenyl-3-methyl-5-pyrazolone (PMP) and 3-(4, 5-dimethylthiazol-2-yl)-2, 5-diphenyl tetrazolium bromide (MTT) and was from sigma-Aldrich, USA. Dextran standards were purchased from Pharmacia Co., Sweden. Acetonitrile and Dimethyl Sulfoxide (DMSO) were purchased from E. Merck, Germany. DEAE-Cellulose 32 was from Whatman Co., U.K. Matrigel with growth factors (354234) was purchased from BD Biosciences, USA. Other reagents were analytical grade.

2.2. General analysis

Total sugar content was determined by the phenol–sulfuric acid method using galactose as standard (Dubois, Gilles, Hamilton, Rebers & Smith, 1956). The content of protein was determined by the Lowry method (Lowry, Rosebrough, Farr & Randall, 1951). Monosaccharide composition of polysaccharides was determined by a PMP-HPLC method according to our previous report (Wang et al., 2014).

2.3. Extraction, isolation and purification of polysaccharides

Extraction of crude polysaccharides was performed by the previous procedure (Wang et al., 2014). In brief, the dried flowers of *Panax notoginseng* was extracted with boiling water for 5 h (5 times). The combined supernatant was concentrated and treated with 15% trichloroacetic acid at 4 °C for 4 h to remove the protein. After neutralization and centrifugation, the supernatant was dialyzed (3500 Da, MWCO), concentrated and precipitated with three volumes of 95% EtOH. The crude polysaccharide RN was fractionated on a DEAE-cellulose column (Cl–, 120 cm × 6 cm), eluted with distilled water and further 0.1 M NaCl. The fraction with 0.1 M NaCl elution was collected, concentrated and lyophilized to obtain polysaccharide RN1. The relative molecular weight of RN1 was determined by HPGPC with series-connected Ultrahydrogel TM 2000 and Ultrahydrogel TM 500 columns and it was estimated to be 20.5 kDa.

2.4. Methylation analysis

The vacuum-dried polysaccharide (10 mg) was methylated for 3-4 times based on previous methods (Hakomori, 1964). The methylated polysaccharide was

hydrolyzed and then reduced with sodium borohydride and acetylated. The partially methylated alditol acetates were analyzed by gas chromatography-mass spectrometry (GC-MS) with a Shimadzu QP-5050A apparatus equipped with a DB-1 capillary column (0.25 mm × 30 m). Mass spectra of the derivatives were analyzed using Complex Carbohydrate Structural Database of Complex Carbohydrate Research Centre (http://www.ccrc.uga.edu/).

2.5. NMR analysis

For NMR analysis, polysaccharides (30 mg) were exchanged and dissolved in 0.5 ml of D_2O. The ^{1}H-, ^{13}C-NMR spectra, two-dimensional spectra (HMBC, HMQC and COSY) were measured at room temperature with acetone as internal standard. NMR spectra were recorded on a Varian Mercury 500 NMR spectrometer.

2.6. Partial acid hydrolysis

RN1 (200 mg) was first hydrolyzed in 0.05 M TFA at 100 °C for 1 h and then evaporated to remove TFA. After dialysis, the retentate was lyophilized to obtain the degraded polysaccharide RN1N1. RN1N1 was further hydrolyzed in 0.1 M TFA at 100 °C for 1 h, then evaporated and dialyzed. The retentate was freeze-dried, giving RN1N2. The monosaccharide composition, molecular weight and NMR analysis were performed for the degraded polysaccharides.

2.7. Cell Lines and Culture Conditions

Human microvascular endothelial cells (HMEC-1) were purchased from Prime Gene Bio-Tech Co. Ltd., Shanghai and maintained in MCDB131 (Gibco BRL, U.S.A.) medium containing 15% FBS (v/v), 2 mM L-glutamine, 10 ng/ml EGF (Shanghai Prime Gene Bio-Tech Co. Ltd., Shanghai, China) and 100 U/ml penicillin, 100 μg/ml streptomycin. Human pancreatic cancer cell lines BxPC-3 were purchased from the Cell Bank in the Type Culture Collection Center in Chinese Academy of Sciences, Shanghai, China. These cells were cultured in RPMI-1640 medium supplemented with 10% fetal bovine serum (FBS) and 1% penicillin/streptomycin. The cells were cultured in an incubator at 37 °C under a humidified atmosphere containing 5% CO_2.

2.8. Cell proliferation (MTT) assay

Cell proliferation was measured by an MTT tetrazolium assay. Briefly, HMEC-1 (4×10^3 cells/well) cells were seeded into 96-well tissue culture plates and cultured with or without RN1. After 72 h, tetrazolium salt was added and the cells were incubated at 37 °C for another 4 h. The insoluble violet formazan product was solubilized by the addition of 150 µl of DMSO. The color absorbance was recorded at 490 nm using a Bio-Rad 3350 micro plate reader. The effect of RN1 on cell viability was calculated in terms of percent of control, which was arbitrarily assigned a value of 100% viability.

2.9. Tube formation assay

A HMEC-1 cells capillary-like tube formation assay was performed to determine the effect of the RN1 on angiogenesis *in vitro*. A total of 5×10^4 HMEC-1 cells were seeded on top of matrigel-coated (40 µl per well) wells of 96-well tissue culture plates containing 0.5 mg/ml, 1 mg/ml of RN1. The plate was then incubated at 37 °C and the formation of the capillary-like tubes was observed after 8 h. The wells were imaged using a Nikon microscope. Quantification of tube formation was assisted by Image-Pro Plus software.

2.10. Wound healing assay

To assess the effect of RN1 on mobility of HMEC-1 cells, a wound healing assay was performed. A total of 5×10^5 HMEC-1 cells were seeded in 6-well plates and incubated in FBS-free MCDB131 for 24 h. An artificial wound was then created, and the cells were washed and supplied with new medium containing 1% FBS and various concentrations of RN1. The migration of cells through the wound area was examined after 0 h, 6 h, 12 h and 24 h.

2.11. Western blotting

Total proteins were extracted and the concentration was determined using the bicinchoninic acid protein assay kit (Beyotime). The total cellular protein extracts were separated by electrophoresis on SDS-PAGE gels and blotted onto the nitrocellulose membrane (Millipore). Blots were incubated with antibodies raised against, Id-1 (Santa Cruz), phospho-Smad1/5/8 (Cell Signaling Technology), β-actin

(Santa Cruz). Protein bands were detected by incubation with HRP-conjugated secondary antibodies, and visualized with enhanced chemiluminescence reagent (Pierce).

2.12. Xenograft model and Immunohistochemistry

Five-week-old female athymic nude (nu/nu) mice were purchased from Shanghai Laboratory Animal center of the Chinese Academy of Sciences. The study was approved by our Institution Animal Care and Use Committee (IACUC). Tumors were established by injecting 5×10^6 BxPC-3 cells subcutaneously into the left flank of mice. Xenograft animals were administrated orally with RN1 dose at 0.5 mg/kg and 20 mg/kg respectively, whereas control animals received equivalent volumes of normal saline. RN1 treatment was initiated when tumors were palpable and continued 46 days. On day 46, the animals were euthanized, and the tumors were excised. The tumors were fixed in 4% paraformaldehyde and then were embedded in paraffin and sectioned for immunohistochemical analysis. Endothelial cells were identified by immunostaining with an antibody against CD31 (abcam). Microvascular density (MVD) was calculated by quantifying CD31-positive microvessels per field of view.

Statistical Analysis

Results are presented as mean values ± standard error. Values of $P < 0.05$ were considered to be statistically significant (* $P < 0.05$, ** $P < 0.01$, *** $P < 0.001$). Statistical analyses were performed by Student *t*-test for comparison of two groups or one-way analysis of variance for multiple comparisons using PRISM software (GraphPad Sofware).

3. RESULTS

3.1 Isolation and composition analysis of RN1

RN1 (5.0% of the crude polysaccharide RN) was isolated on a DEAE-cellulose column eluted with 0.1 M NaCl. Its homogeneity was estimated by HPGPC, in which it showed one symmetrical peak. The relative molecular weight of RN1 was estimated to be 20.5 kDa. The results showed that RN1 contained no protein by the Lowry method. Monosaccharide composition analysis indicated that RN1 mainly contained

Gal (43.7%) and Ara (56.3%).

3.2 Methylation analysis

To determine the glycosyl linkage type, RN1 was methylated and hydrolyzed and then the partially methylated alditol acetates (PMAA) were analyzed by GC-MS (Table 1). The nonreducing terminals consisted of Ara*f* (12.63%) and a small amount of Gal*p* (6.87%). The intrachains residues were 1,3 linked Gal*p* (19.73%), 1,6 linked Gal*p* (29.42%) and 1,5 linked Ara*f* (18.19%). The main branching points were at 1,3,5-linked Ara*f* (8.06%) and 1,3,6-linked Gal*p* (9.10%). These results indicated that RN1 was significantly branched.

3.3 Partial acid hydrolysis

To determine the detailed structure of RN1, it was partially hydrolyzed with 0.05 M TFA and the hydrolysate were dialyzed, giving RN1N1 (nodialysate) and RN1F1 (dialysate). The GPC results showed that RN1N1 was homogeneous with an *Mw* of 10.9 kDa, indicating it was significantly degraded. The results of monosaccharides composition analysis showed that RN1N1 was composted of Gal (64.6%) and Ara (35.4%). RN1F1 contained monosaccharides and oligosaccharides with composed of Gal (27.9%) and Ara (72.1%). These results indicated that the Ara residues were more sensitive than Gal residues to this mild acid, probably due to their linkages and location in the outer branches. Methylation analysis (Table 1) showed that total ratio of Ara residues of RN1N1 were decreased than that of native RN1, as along with the 1,3,5-linked Ara*f* disappeared. To further determine the structural features, RN1N1 was hydrolyzed in 0.1 M TFA at 100 °C for 1 h, giving RN1N2 (nodialysate). RN1N2 was mainly composed of Gal, with an *Mw* of 6.9 kDa, indicating all of Ara residues were removed as monosaccharides or oligosaccharides by mild hydrolysis. These data suggested that RN1 probably contained a galactan backbone with Ara distributed in the outer branches. Methylation analysis (Table 1) showed that the molar ratio of 1,6/ l,3,6/T-linked Gal*p* of RN1N2 were 3:1:1, which indicated that every four 1,6-linked Gal was substituted at O-3 with one Gal residue in the core structure of RN1, and then the linkage of branched Gal was 1,3-linked, according to methylation results of RN1 and RN1N1. These results indicated that RN1 had a backbone structure of 1,6-linked

Gal*p* branched at C3 by side 1,3-linked Gal*p*.

3.4 NMR results

In the ^{13}C-NMR spectrum of native RN1 (Fig. 1A), the anomeric signals of Ara and Gal were easily assigned combined with the ^{13}C-NMR spectra of two-step degraded fractions of RN1N1 (Fig. 1B) and RN1N2 (Fig. 1C), according to monosaccharides composition, methylation results and previous literature data. The signals of δ110.84, δ110.57 and δ109.57 were assigned to the anomeric carbons of α-L-T-Ara*f*, α-L-1,5-Ara*f* and α-L-1,3,5-Ara*f*, while the signals at δ105.01, δ104.65 and δ104.26 were attributed to the anomeric carbons of β-D-1,3/1,3,6-Gal*p*, β-D-1,6-Gal*p* and β-D-T-Gal*p*, respectively (Capek, Matulova, Navarini & Suggi-Liverani, 2010; de Oliveira, Cordeiro, Goncalves, Ceole, Ueda-Nakamura & Iacomini, 2013; Dong et al., 2010; Xu, Dong, Qiu, Cong & Ding, 2010). The overlap signals at δ70.0-δ70.1 were ascribed to C5 of 1,5/1,3,5-linked Ara and C6 of 1,6/1,3,6-linked Gal, whereas the obvious double-peak at δ62.1 was from unsubstituted C6 of Gal and C5 of Ara, respectively. The anomeric signals in the ^{1}H-NMR spectra of RN1 and RN1N2 were assigned mainly according to the carbon and hydrogen correlations in the HSQC and HMBC (Fig. 2). The signal at δ5.43 was assigned to α-L-1,3,5-Ara*f* residue, and the overlapping peaks at δ5,25 were from α-L-1,5/T-Ara*f* residues (Fig. 2A). The obvious overlapping peaks at δ4.52 could be attributed to β-D-1,3/1,3,6/1,6/T-Gal*p* residues (Fig. 2A and Fig. 2C). In the HMBC spectrum of RN1N2 (Fig. 2D), the transglycosidic correlation between H1 (δ4.51) of 1,3,6-linked Gal and substituted Gal C6 (δ70.55), indicating a probable 1,6-linked galactan backbone in the arabinogalactan structure. Other signals of RN1 were assigned in reference to values found in previous literature or according to HSQC and HMBC (Fig. 2), and the results were shown in Table 2.

Taken together, RN1 was an neutral arabinogalactan with a galactan backbone composed of every four 1,6-linked Gal*p* residues branched at O-3 by side 1,3-linked Gal*p*. The branches mainly occurred at O-3 of 1,3-linked Gal*p* and consisted of T/1,5/1,3,5-linked Ara residues or T-linked Gal residues. The presence of 1,3,5-linked

Ara indicated that RN1 had a branched structure composed of 1,5-linked Ara residues substituted at O-3 by terminal arabinose residues. Hence, the putative core structure of RN1 was deduced as followed:

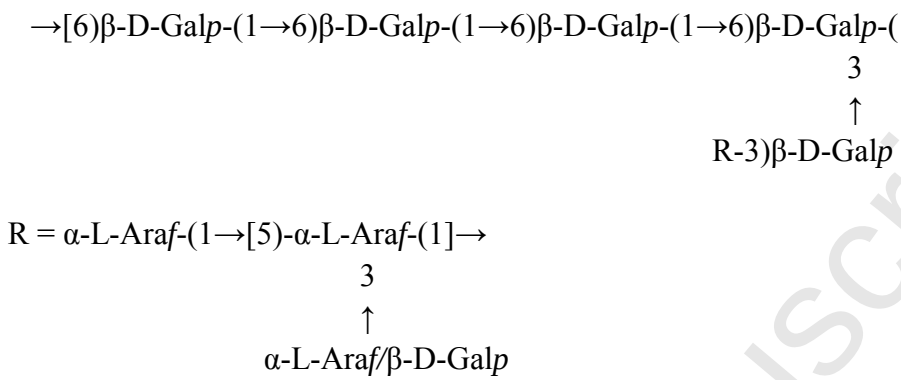

3.5 RN1 inhibited HMEC-1 tube formation and migration

Angiogenesis is a highly regulated process of new blood vessel formation from pre-existing vessels. It is essential for tumor metastasis, while endothelial cells migration and tube formation is essential for angiogenesis (Folkman & Shing, 1992). To detect the inhibitory effects of angiogenesis, HMEC-1 tube formation assays in the presence of RN1 *in vitro* were performed. Non-reduced matrigel with complete media was used in this experiment, due to its promotion of robust tube formation. As shown in Fig. 3A and 3B, RN1 (0.5 mg/ml) significantly reduced the number of branch points and tube numbers, it could disrupted the enclosed capillary network completely at the concentration of 1 mg/ml.

As endothelial cells tube formation is only one fact of angiogenesis, to determine whether RN1 can inhibit other aspects of new blood vessel development, HMEC-1 cells wound healing assay *in vitro* was also performed. Tight monolayers of the cells were damaged to provoke cell migration into the wound area. As shown in Fig. 3C and 3D, the migration of the HMEC-1 cells was substantially inhibited after RN1 treatment compared with the control as quantified by measuring the area of the wound covered.

To confirm that the inhibitory effects of tube formation and migration is not the results of HMEC-1 cells proliferation inhibition, the viability of HMEC-1 after RN1 treatment was measured. As shown in Fig. 3E, RN1 had no significant effect on viability of HMEC-1 cells.

Collectively, these results suggested that RN1 could inhibit angiogenesis *in vitro*.

3.6 RN1 inhibit BMP2 signaling

Bone morphogenetic proteins (BMPs), members of the transforming growth factor (TGF)-β super family, are known to modulate various cellular processes, including proliferation, apoptosis, differentiation and migration (Jin et al., 2012). Our previous studies showed that BMP2 signaling was associated with angiogenesis inhibition induced by polysaccharides (Qiu, Yang, Pei, Zhang & Ding, 2010; Xiao, Qiu, Zhou, Shen, Yang & Ding, 2013). To explore whether the anti-angiogenesis effects of RN1 were linked to BMP2 signaling, we firstly analyzed the phosphorylation level of Smad1/5/8. As shown in Figure 4A, RN1 could decrease the phosphorylation of Samd1/5/8 after incubation with RN1 for 4 h. We then determined whether RN1 could affect Id-1 expression, as Id-1 is the BMP2 downstream target gene of BMP2 signaling. As shown in Fig. 4B, RN1 could attenuate Id-1 expression in a time-dependent manner (Fig. 4B). Id-1 is well established as an anti-angiogenesis target, partial loss of Id-1 by genetic manipulation in mice effectively inhibits tumor angiogenesis (Lyden et al., 1999). BMPs mediated Id-1 gene expression via modulating the phosphorylation of Smad1/5/8, which formed a complex with Smad4 after the phosphorylation and then translocated into the nucleus to modulate Id1 expression (Kawabata, Imamura & Miyazono, 1998; Valdimarsdottir et al., 2002). Indeed, RN1 effectively blocked the BMP2 induced Id-1 expression, similar to the effect of the endogenous BMP2 antagonist noggin used as a control (Fig. 4C). These results suggested that RN1 down-regulated Id-1 expression might be through inhibiting BMP2 signaling in HMEC-1 cells.

3.7 RN1 suppresses the growth of pancreatic cancer xenograft in nude mice.

To evaluate the anti-angiogenesis effect of RN1 *in vivo*, we employed the BxPC-3 pancreatic cancer cell line xenograft tumor model. We assessed microvessel formation in the xenografts by staining for the endothelial marker CD31. Then we found that the average microvessel number in the xenografts of the RN1 treatment was significantly less than that of the control group (Fig. 5). These results indicated RN1 exerted a significant anti-angiogenesis activity *in vivo*.

DISCUSSION

Arabinogalactans (AGs) are structural complex branched polysaccharides, widely present in plant cell walls. According to the structure features, AGs are generally classified into two main types. Types Ⅰ AGs have a linear 1,4-lined galactan backbone with Ara substituted by O-3 of galactose residues in main chains (Mellinger et al., 2005; Xu, Dong, Qiu, Cong & Ding, 2010). Type Ⅱ AGs usually contain a 1,3-linked galactan backbone with 1,6-linked galactan side chains. The galactose residues can be further substituted with 1,5/1,3,5/terminal-linked Ara (Dong, Hayashi, Lee & Hayashi, 2010; Nergard et al., 2005; Tryfona, Liang, Kotake, Tsumuraya, Stephens & Dupree, 2012). In the present study, a novel arabinogalactan RN1 was isolated and purified from FPN, which differed from those reported studies about other arabinogalactan (Lee, Li, Chatterjee & Lee, 2005; Mellinger et al., 2005; Nergard et al., 2006; Suarez et al., 2005; Tryfona, Liang, Kotake, Tsumuraya, Stephens & Dupree, 2012; Wack, Classen & Blaschek, 2005; Xu, Dong, Qiu, Cong & Ding, 2010). Although the structure of RN1 is similar with SFW-10RM and SSFK-10RM isolating from *Stevia rebaudiana* leaves, RN1 has anti-angiogenesis activity, while SFW-10RM and SSFK-10RM showed anti-virus activity (de Oliveira, Cordeiro, Goncalves, Ceole, Ueda-Nakamura & Iacomini, 2013).

It was well known that heparan sulfate (HS) could bind multiple functional proteins including pro-angiogenic factors such as VEGF and FGF2, through which they can mediate angiogenic signaling, due to their negative charges. Then HS mimetics are widely reported to inhibit angiogenesis by blocking the interaction between angiogenic factors and their receptors (Forsten-Williams, Chua & Nugent, 2005; Fujita et al., 2010). For example, our group previously reported that WSS25, a sulfated derivative of glucan could inhibit angiogenesis *in vitro and in vivo* (Qiu, Yang,

Pei, Zhang & Ding, 2010). However, in the animal safety experiment, we found that WSS25 at high concentration could increase the chances of internal bleeding, probably due to high degree of sulfation. To find more safety antiangiogenic inhibitors, we searched for new modulators of angiogenesis from natural products. To our knowledge, there are some reports about the arabinogalactans polysaccharides with the activity of anti-virus (Saha et al., 2010), immunomodulation (Choi, Kim, Kim & Hwang, 2005) and anti-proliferation in tumor cells (Bento, Noleto & de Oliveira Petkowicz, 2014), however, there are few reports about arabinogalactans polysaccharide with the anti-angiogenesis activity. We previously reported that PGAW1 (Xu, Dong, Qiu, Cong & Ding, 2010), an arabinogalactan from *Platycodon grandiflorum* Roots, containing a 1, 4-D-Galp backbone, has no effect on HMEC-1 tube formation at the concentration of 100 μg/ml. However, the sulfated derivative showed a strong dose-dependent anti-angiogenesis activity compared to that of PGAW1. Here, we reported for the first time that RN1, as a neutral polysaccharide, was determined to have a 1, 6-linked galactan backbone, besides, RN1 contains branches with arabinose, which differed from PGAW1 and was not sulfated, but showed distinct anti-angiogenesis activity *in vitro* and *in vivo*. Further studies of anti-angiogenesis mechanism showed that RN1 could inhibit BMP2 signaling. Hence we think the activity was mainly attributed to the novel structures of RN1. Our findings suggested that RN1 could be a potential novel inhibitor of angiogenesis and had therapeutic potential development in tumor angiogenesis.

Acknowledgments:

This work was supported by grants from National Natural Science Foundation of China (31230022), New Drug Creation and Manufacturing Program (2012ZX09301001-003), National Science Fund for Distinguished Young Scholars in China (81125025), and Shanghai Research Program (13ZR1447500).

Conflicts of Interest

The authors declare that they have no conflicts of interest concerning this article.

REFERENCES

Bento, J. F., Noleto, G. R., & de Oliveira Petkowicz, C. L. (2014). Isolation of an arabinogalactan from Endopleura uchi bark decoction and its effect on HeLa cells. *Carbohydr Polym, 101*, 871-877.

Capek, P., Matulova, M., Navarini, L., & Suggi-Liverani, F. (2010). Structural features of an arabinogalactan-protein isolated from instant coffee powder of Coffea arabica beans. *Carbohydrate Polym, 80*(1), 180-185.

Choi, E. M., Kim, A. J., Kim, Y. O., & Hwang, J. K. (2005). Immunomodulating activity of arabinogalactan and fucoidan in vitro. *J Med Food, 8*(4), 446-453.

de Oliveira, A. J., Cordeiro, L. M., Goncalves, R. A., Ceole, L. F., Ueda-Nakamura, T., & Iacomini, M. (2013). Structure and antiviral activity of arabinogalactan with (1-->6)-beta-D-galactan core from Stevia rebaudiana leaves. *Carbohydr Polym, 94*(1), 179-184.

Dong, C. X., Hayashi, K., Lee, J. B., & Hayashi, T. (2010). Characterization of structures and antiviral effects of polysaccharides from Portulaca oleracea L. *Chem Pharm Bull (Tokyo), 58*(4), 507-510.

Dong, Q., Liu, X., Yao, J., Dong, X., Ma, C., Xu, Y., Fang, J., & Ding, K. (2010). Structural characterization of a pectic polysaccharide from Nerium indicum flowers. *Phytochemistry, 71*(11-12), 1430-1437.

Dubois, M., Gilles, K. A., Hamilton, J. K., Rebers, P. A., & Smith, F. (1956). Colorimetric Method for Determination of Sugars and Related Substances. *Analytical Chemistry, 28*(3), 350-356.

Folkman, J., & Shing, Y. (1992). Angiogenesis. *J Biol Chem, 267*(16), 10931-10934.

Forsten-Williams, K., Chua, C. C., & Nugent, M. A. (2005). The kinetics of FGF-2 binding to heparan sulfate proteoglycans and MAP kinase signaling. *J Theor Biol, 233*(4), 483-499.

Fujita, K., Takechi, E., Sakamoto, N., Sumiyoshi, N., Izumi, S., Miyamoto, T., Matsuura, S., Tsurugaya, T., Akasaka, K., & Yamamoto, T. (2010). HpSulf, a heparan sulfate 6-O-endosulfatase, is involved in the regulation of VEGF signaling during sea urchin development. *Mech Dev, 127*(3-4), 235-245.

Hakomori, S. (1964). A Rapid Permethylation of Glycolipid, and Polysaccharide Catalyzed by Methylsulfinyl Carbanion in Dimethyl Sulfoxide. *J Biochem, 55*, 205-208.

Hanahan, D., & Weinberg, R. A. (2011). Hallmarks of cancer: the next generation. *Cell, 144*(5), 646-674.

Jin, H., Pi, J., Huang, X., Huang, F., Shao, W., Li, S., Chen, Y., & Cai, J. (2012). BMP2 promotes migration and invasion of breast cancer cells via cytoskeletal reorganization and adhesion decrease: an AFM investigation. *Appl Microbiol Biotechnol, 93*(4), 1715-1723.

Kawabata, M., Imamura, T., & Miyazono, K. (1998). Signal transduction by bone morphogenetic proteins. *Cytokine Growth Factor Rev, 9*(1), 49-61.

Lee, R. E., Li, W., Chatterjee, D., & Lee, R. E. (2005). Rapid structural characterization of the arabinogalactan and lipoarabinomannan in live mycobacterial cells using 2D and 3D HR-MAS NMR: structural changes in the arabinan due to ethambutol treatment and gene mutation are observed. *Glycobiology, 15*(2), 139-151.

Lowry, O. H., Rosebrough, N. J., Farr, A. L., & Randall, R. J. (1951). Protein Measurement with the Folin Phenol Reagent. *J Biol Chem, 193*(1), 265-275.

Lyden, D., Young, A. Z., Zagzag, D., Yan, W., Gerald, W., O'Reilly, R., Bader, B. L., Hynes, R. O., Zhuang, Y., Manova, K., & Benezra, R. (1999). Id1 and Id3 are required for neurogenesis, angiogenesis and vascularization of tumour xenografts. *Nature, 401*(6754), 670-677.

Mellinger, C. G., Carbonero, E. R., Noleto, G. R., Cipriani, T. R., Oliveira, M. B., Gorin, P. A., & Iacomini, M. (2005). Chemical and biological properties of an arabinogalactan from Phyllanthusniruri. *J Nat Prod, 68*(10), 1479-1483.

Nergard, C. S., Kiyohara, H., Reynolds, J. C., Thomas-Oates, J. E., Matsumoto, T., Yamada, H., Michaelsen, T. E., Diallo, D., & Paulsen, B. S. (2005). Structure-immunomodulating activity relationships of a pectic arabinogalactan from Vernonia kotschyana Sch. Bip. ex Walp. *Carbohydr Res, 340*(11), 1789-1801.

Nergard, C. S., Kiyohara, H., Reynolds, J. C., Thomas-Oates, J. E., Matsumoto, T., Yamada, H., Patel, T., Petersen, D., Michaelsen, T. E., Diallo, D., & Paulsen, B. S. (2006). Structures and structure-activity relationships of three mitogenic and complement fixing pectic arabinogalactans from the malian antiulcer plants Cochlospermum tinctorium A. Rich and Vernonia kotschyana Sch. Bip. ex Walp. *Biomacromolecules, 7*(1), 71-79.

Ng, T. B. (2006). Pharmacological activity of sanchi ginseng (Panax notoginseng). *J Pharm Pharmacol, 58*(8), 1007-1019.

Qiu, H., Yang, B., Pei, Z. C., Zhang, Z., & Ding, K. (2010). WSS25 inhibits growth of xenografted hepatocellular cancer cells in nude mice by disrupting angiogenesis via blocking bone morphogenetic protein (BMP)/Smad/Id1 signaling. *J Biol Chem, 285*(42), 32638-32646.

Saha, S., Galhardi, L. C., Yamamoto, K. A., Linhares, R. E., Bandyopadhyay, S. S., Sinha, S., Nozawa, C., & Ray, B. (2010). Water-extracted polysaccharides from Azadirachta indica leaves: Structural features, chemical modification and anti-bovine herpesvirus type 1 (BoHV-1) activity. *Int J Biol Macromol, 47*(5), 640-645.

Suarez, E. R., Kralovec, J. A., Noseda, M. D., Ewart, H. S., Barrow, C. J., Lumsden, M. D., & Grindley, T. B. (2005). Isolation, characterization and structural determination of a unique type of arabinogalactan from an immunostimulatory extract of Chlorella pyrenoidosa. *Carbohydr Res, 340*(8), 1489-1498.

Tryfona, T., Liang, H. C., Kotake, T., Tsumuraya, Y., Stephens, E., & Dupree, P. (2012). Structural characterization of Arabidopsis leaf arabinogalactan polysaccharides. *Plant Physiol, 160*(2), 653-666.

Valdimarsdottir, G., Goumans, M. J., Rosendahl, A., Brugman, M., Itoh, S., Lebrin, F., Sideras, P., & ten Dijke, P. (2002). Stimulation of Id1 expression by bone morphogenetic protein is sufficient and necessary for bone morphogenetic protein-induced activation of endothelial cells. *Circulation, 106*(17), 2263-2270.

441 Wack, M., Classen, B., & Blaschek, W. (2005). An acidic arabinogalactan-protein
442 from the roots of Baptisia tinctoria. *Planta Med, 71*(9), 814-818.
443 Wang, P., Liao, W., Fang, J., Liu, Q., Yao, J., Hu, M., & Ding, K. (2014). A glucan
444 isolated from flowers of Lonicera japonica Thunb. inhibits aggregation and
445 neurotoxicity of Abeta42. *Carbohydr Polym, 110*, 142-147.
446 Weis, S. M., & Cheresh, D. A. (2011). Tumor angiogenesis: molecular pathways and
447 therapeutic targets. *Nat Med, 17*(11), 1359-1370.
448 Xiao, F., Qiu, H., Zhou, L., Shen, X., Yang, L., & Ding, K. (2013). WSS25 inhibits
449 Dicer, downregulating microRNA-210, which targets Ephrin-A3, to suppress human
450 microvascular endothelial cell (HMEC-1) tube formation. *Glycobiology, 23*(5),
451 524-535.
452 Xu, Y., Dong, Q., Qiu, H., Cong, R., & Ding, K. (2010). Structural characterization of
453 an arabinogalactan from Platycodon grandiflorum roots and antiangiogenic activity of
454 its sulfated derivative. *Biomacromolecules, 11*(10), 2558-2566.
455
456

Figure legend

Figure 1. ^{13}C-NMR spectra of RN1 (A), RN1N1 (B) and RN1N2(C).

Figure 2. 2D-NMR spectra of RN1 and RN1N2.

A. HSQC spectrum of RN1; B. HMBC spectrum of RN1; C. HSQC spectrum of RN1N2; D. HMBC spectrum of RN1N2. "a" means "intra-annular correlation" and "b" means "hetero-ring correlation" in Fig 2b and 2d.

Figure 3. RN1 impaired the tube formation of HMEC-1 cells on matrigel and migration.

A. HMEC-1 cells treated with RN1 at different concentration (0.5 mg/ml, 1 mg/ml) or vehicle (control) were seeded into the 96-well plate pre-coated with 40 μl matrigel. Representative image of tube formation after 8 h of culturing (40 ×). B. Quantitative measurement of tube formation. C. HMEC-1 monolayer was scraped to generate a wound (0 h), and the cells were incubated with different concentration of RN1 (0.5 mg/ml, 1 mg/ml) or vehicle (Control), after 12 h, the cells were imaged at 40 × magnification. The wound areas at time 0 and 12 are indicated by dotted lines. D. Quantification of effect of RN1 on HMEC-1 cells migration in the wound healing assay. E. HMEC-1 cells were seed into 96 well plates, after 24 h of incubation, RN1 was added to the final concentration of 0.25 mg/ml, 0.5 mg/ml, 1 mg/ml. The cell viability was determined by the MTT assay 72 h later. Each experiment was performed at least 3 times, and the values represent mean ± S.D. *, $P < 0.05$; **, $P < 0.01$, as determined by unpaired Student's *t*-test.

Figure 4. RN1 inhibited BMP2 signaling pathway.

A. B. The HMEC-1 cells were incubated with 1 mg/ml of RN1 for indicated times, the expression of Smad 1/5/8 phosphorylation and Id-1 were analyzed by western blotting. β-actin was used as loading control. C. HMEC-1 cells were pretreated with 1mg/ml of RN1, 5 μg/ml noggin or vehicle for 23 h, the cells were then treated with 50 ng/ml of BMP2 or vehicle for another hour, the extracted proteins were analyzed by western blotting. β-actin was used as loading control.

Figure 5. RN1 inhibited angiogenesis *in vivo*.

A. Tumor sections were stained with anti-CD31. Representative image of the Immunohistochemical analysis (200 ×). Arrows indicate CD31-positive vessels. B. Microvascular counting was performed using Image Pro Plus. Results are presented as means ± S.D.. *, $P < 0.05$; **, $P < 0.01$, as determined by unpaired Student's *t*-test.

Highlight

1. A novel arabinogalactan RN1 was isolated and purified from flowers of *Panax notoginseng*.
2. The structure of RN1 was determined to possess a backbone of 1,6-linked Gal*p* branched at C3 by side 1,3-linked Gal*p*, with branches attached at position O-3 of it.
3. RN1 could inhibit angiogenesis by BMP2/ Smad1/5/8/Id1 signaling.

Table 1 Linkage analysis of RN1 by GC-MS

Methylated sugars	Linkages	Molar ratio (%)		
		RN1	RN1N1	RN1N2
2,3,5- Me_3-Ara*f*	Terminal-Ara*f*	12.63	9.4	-
2,3- Me_2-Ara*f*	1,5-Ara*f*	21.19	19.93	-
2- Me-Ara*f*	1,3,5-Ara*f*	10.06	-	-
2,3,4,6-Me_4-Gal*p*	Terminal-Gal*p*	6.87	10.53	20.97
2,4 ,6-Me_3-Gal*p*	1,3-Gal*p*	10.73	11.29	-
2,3,4-Me_3-Gal*p*	1,6-Gal*p*	29.42	36.17	58.54
2,4- Me_2-Gal*p*	1,3,6-Gal*p*	9.10	12.68	20.49

Table 2 ^{1}H and ^{13}C-NMR Spectral assignments for RN1

Residues		1	2	3	4	5	6
T-α-Ara*f*	H	5.25	4.21	3.92	4.12	3.83	
	C	110.84	82.54	77.90	85.15	62.34	
1,5-α-Ara*f*	H	5.24	4.21	3.92	4.11	3.93	
	C	110.57	82.54	77.90	85.22	70.64	
1,3,5-α-Ara*f*	H	5.43	4.18	3.95	4.11	3.93	
	C	109.57	82.67	78.03	84.82	70.97	
T-β-Gal*p*	H	4.49	3.58	3.71	3.96	4.01	3.82
	C	104.26	71.49	73.38	74.57	69.88	62.19
1,3-β-Gal*p*	H	4.51	3.60	3.74	3.97	4.01	3.82
	C	105.01	72.28	76.54	74.80	69.88	62.10
1,3,6-β-Gal*p*	H	4.51	3.59	3.71	3.97	4.01	4.08
	C	105.01	72.12	76.54	74.84	69.88	70.76
1,6-β-Gal*p*	H	4.52	3.59	3.74	3.98	4.01	4.08
	C	104.65	72.16	73.94	75.09	69.88	70.55

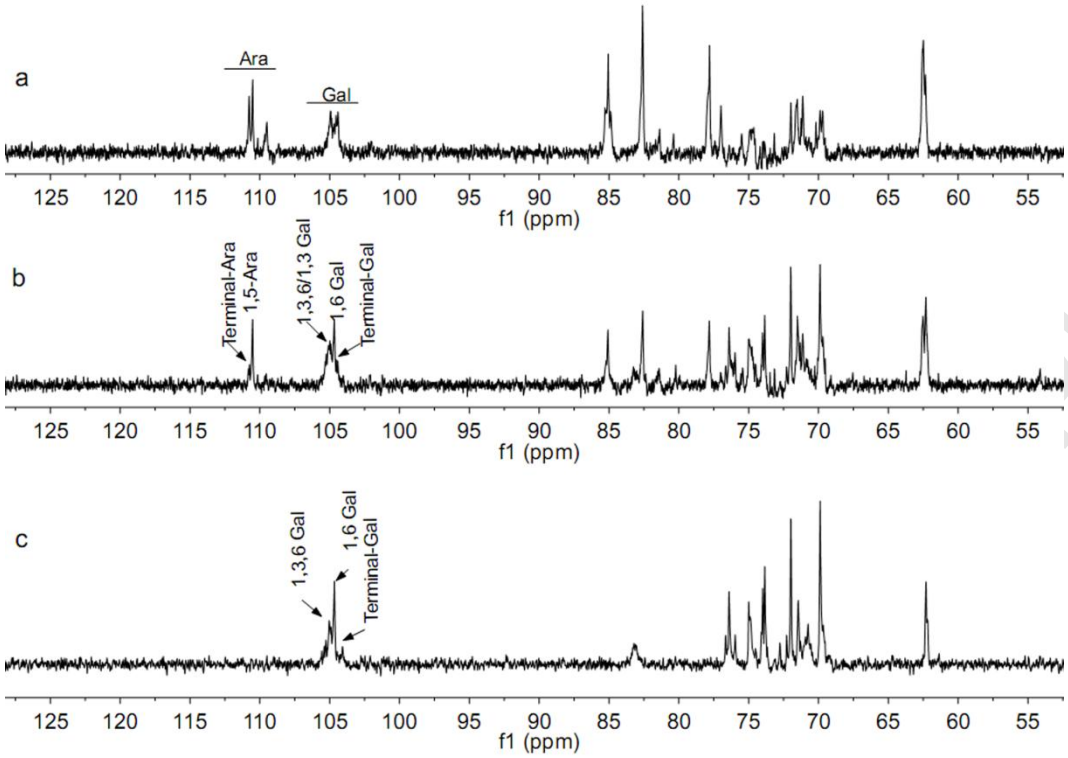

Fig.1

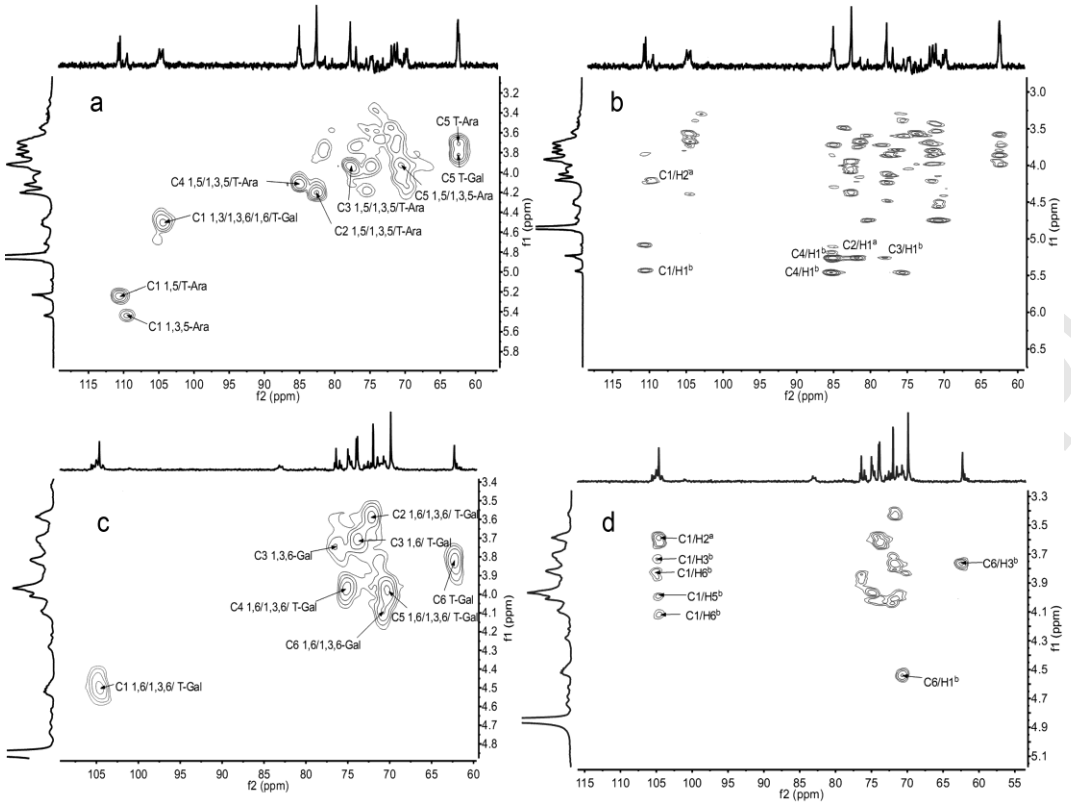

Fig.2

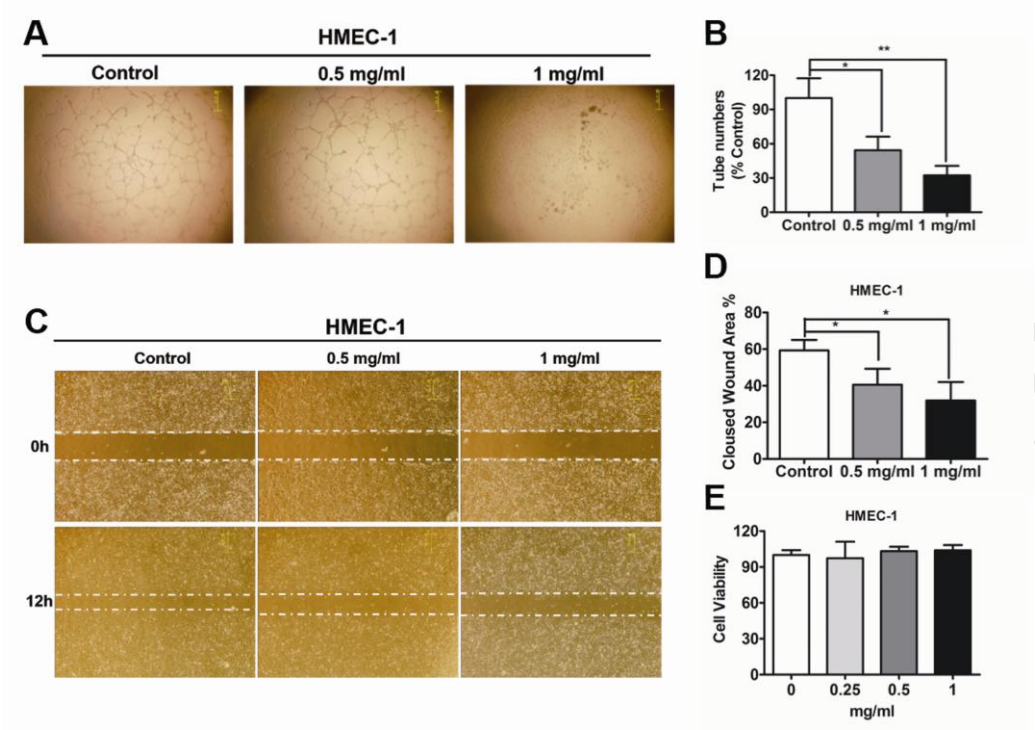

Fig.3

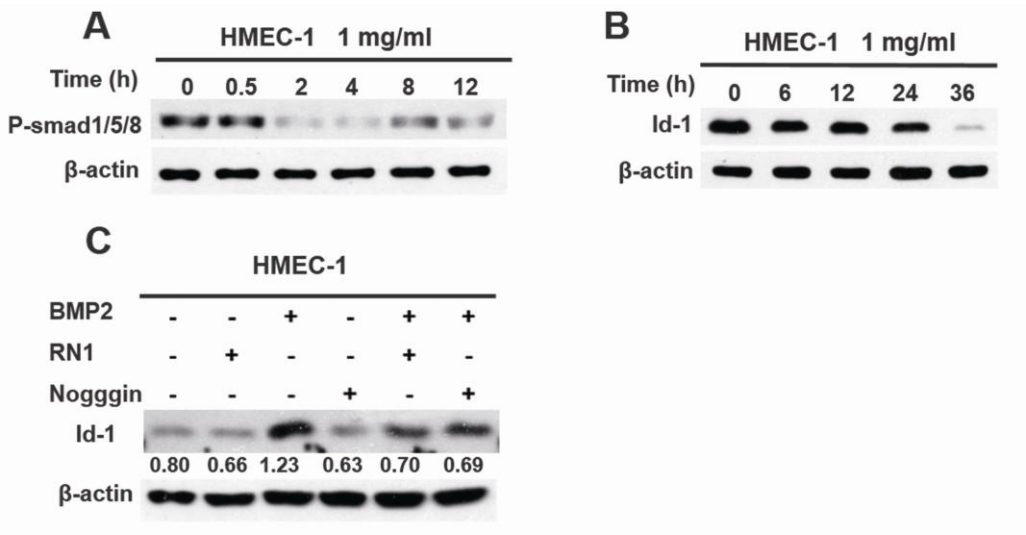

Fig.4

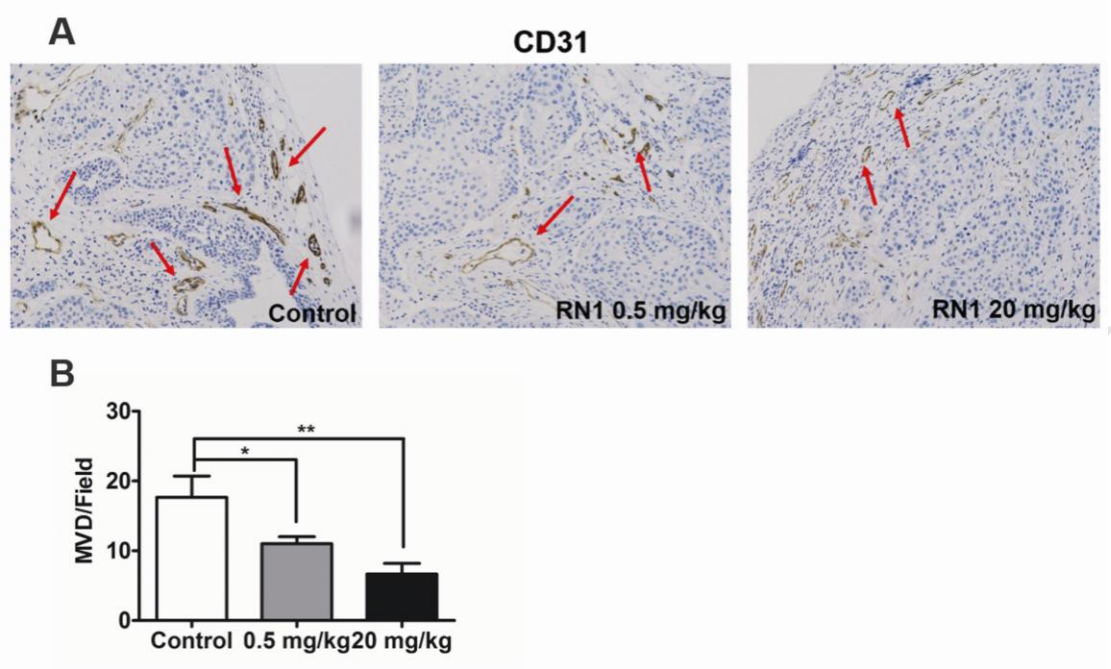

Fig.5